REDUCED AND SELECTIVE INTEGRATION TECHNIQUES IN THE FINITE ELEMENT ANALYSIS OF PLATES *

Thomas J.R. HUGHES, Martin COHEN, Medhat HAROUN

Division of Engineering and Applied Science, California Institute of Technology, Pasadena, California 91125, USA

Efforts to develop effective plate bending finite elements by reduced integration techniques are described. The basis for the development is a 'thick' plate theory in which transverse shear strains are accounted for. The variables in the theory are all kinematic, namely, displacements and independent rotations. As only C^0 continuity is required, isoparametric elements may be employed, which result in several advantages over thin plate elements. It is shown that the avoidance of shear 'locking' may be facilitated by reduced integration techniques. Both uniform and selective schemes are considered. Conditions under which selective schemes are invariant are identified, and they are found to have an advantage over uniform schemes in the present situation. It is pointed out that the present elements are not subject to the difficulties encountered by thin plate theory elements, concerning boundary conditions. For example, the polygonal approximation of curved, simply-supported edges is convergent. Other topics discussed are the equivalence with mixed methods, rank deficiency, convergence criteria and useful mass 'lumping' schemes for dynamics. Numerical results for several thin plate problems indicate the high degree of accuracy attainable by the present elements.

1. Introduction

The 'displacement method' is generally viewed as the most simple and direct basis for finite element developments in structural analysis. However, it has not had unqualified success as the progenitor of thin plate elements. The main difficulty is due to the C^1-continuity requirement of the classical Poisson–Kirchhoff theory, a significant impediment to the derivation of elements. Many ingenious schemes have been devised, and alternative formulations proposed, yet the attainment of simplicity, accuracy and generality in a single element has proven elusive.

Other problems beleaguer thin plate elements. For example, polygonal approximations to curved, simply-supported boundaries generally result in non-convergent approximations, unless inconvenient modifications are adopted, and non-convergence has been demonstrated for certain singular solutions.

In light of these circumstances, the temptation is

great to abandon the Poisson–Kirchhoff theory in favor of one less beset with intrinsic difficulties. The most suitable starting point seems to be a theory in which the classical hypothesis of zero shear strain is relaxed. If displacement-type variables are to be retained, one is naturally led, in the simplest situation, to the 'thick' plate theory of Mindlin [1]. Several benefits are immediate, namely, greater flexibility in the specification of boundary conditions, which enable the aforementioned difficulties to be circumvented, and only C^0 continuity is required of displacement and rotation variables, which is more easily achieved in a finite element setting.

In this paper we report upon some of our efforts to devise plate bending finite elements based upon Mindlin theory.

In section 2 the general theory is described, starting with basic principles and ending with the definition of the element stiffness matrix and load vector. (The reader who is already familiar with the general theory may wish to skip section 2.)

In section 3 we treat topics pertinent to the development of effective plate elements. The main point one must be aware of is the tendency of elements to

'lock' in thin plate applications. Based upon earlier studies, it is concluded that the Lagrange element family, with reduced shear integration, is the most promising of the standard element families in alleviating this tendency. Both 'uniform' and 'selective' reduced integration elements are proposed, and the issue of invariance is clarified.

Boundary conditions appropriate to the present theory are delineated and problems with the thin plate theory boundary conditions are elaborated on. It is pointed out that the present elements are equivalent to ones derived from a 'mixed' variational formulation. The main shortcoming of the present elements, zero-energy modes, is also discussed.

In section 4, some basic ideas in transient analysis are presented. It is shown how to derive 'lumped', positive-definite, mass matrices which yield large critical time steps for explicit transient calculations. In section 5 numerical examples are presented which indicate the high accuracy attainable by the present elements. Conclusions and recommendations are given in section 6.

2. General Theory

All quantities are referred to a fixed system of rectangular, cartesian coordinates. A general point in this system is denoted by (x_1, x_2, x_3), or (x, y, z), whichever is more convenient. Throughout, Latin and Greek indices take on the values $1, 2, 3$, and $1, 2$, respectively, and the summation convention is employed. A comma is used to denote partial differentiation with respect to spatial coordinates (e.g. $u_{i,j} \equiv \partial u_i / \partial x_j$). The symmetric part of rank-2 tensors is denoted by enclosing the indices in parentheses (e.g. $u_{(i,j)} \equiv (u_{i,j} + u_{j,i})/2$).

2.1. Classical linear elasticity

The starting point of the present theory is with the equations of classical linear elasticity:

$$t_{ij,j} + f_i \equiv 0 \tag{1}$$

$$t_{ij} = c_{ijkl} \epsilon_{kl} \Bigg\} , \qquad \text{in } \Omega, \tag{2}$$

$$\epsilon_{ij} = u_{(i,j)} \tag{3}$$

$$u_i = g_i, \qquad \text{on } \Gamma_1, \tag{4}$$

$$t_i = t_{ij} n_j = h_i \qquad \text{on } \Gamma_2, \tag{5}$$

The notation is as follows:

u_i = displacement vector,

ϵ_{ij} = strain tensor,

t_{ij} = stress tensor,

f_i = applied body force vector (per unit volume),

g_i = prescribed boundary displacement vector,

h_i = prescribed boundary traction vector,

c_{ijkl} = elasticity tensor,

n_i = unit outward normal vector.

The domain Ω is contained in $\mathcal{R}^3$ and bounded by a piecewise smooth surface Γ, which is composed of subdomains Γ_1 and Γ_2, satisfying $\overline{\Gamma_1 \cup \Gamma_2} = \Gamma$ and $\Gamma_1 \cap \Gamma_2 = \emptyset$.

The variational equation (i.e. 'principle of virtual work') of the above theory is

$$\int_\Omega t_{ij} \bar{u}_{(i,j)} \, \mathrm{d}\Omega = \int_\Omega f_i \bar{u}_i \, \mathrm{d}\Omega + \int_{\Gamma_2} h_i \bar{u}_i \, \mathrm{d}\Gamma, \tag{6}$$

in which

$$t_{ij} = c_{ijkl} u_{(k,l)}, \tag{7}$$

$$u_i = g_i \Bigg\} , \qquad \text{on } \Gamma_1. \tag{8}$$

$$\bar{u}_i = 0 \qquad \tag{9}$$

2.2. Main assumptions

The main assumptions of the plate theory are:

(1) The domain Ω is of the following special form:

$$\Omega = \{(x, y, z) \in \mathcal{R}^3 \mid z \in [-t/2, t/2],$$

$$(x, y) \in A \subset \mathcal{R}^2 \},$$

where t is the plate thickness and A is its area. The boundary of A is denoted as s.

(2) $t_{33} = 0$.

(3) $u_\alpha(x, y, z) = -z\theta_\alpha(x, y)$.

(4) $u_3(x, y, z) = w(x, y)$.

Remarks

(a) In assumption (1), we may take the plate thickness t to be a function of x and y, if desired.

(b) Assumption (2) is the plane stress hypothesis. It contradicts assumption (4), but ultimately causes no problem. The justification of the present theory is its usefulness in practical structural engineering applications. No plate theory is completely consistent with the three-dimensional theory and, at the same time,
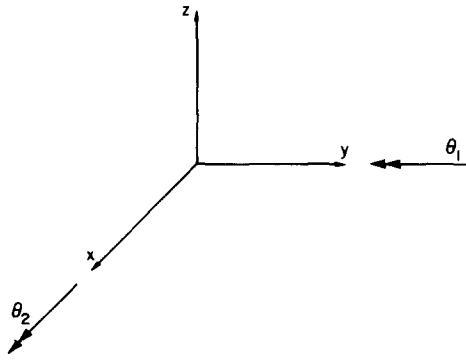
Fig. 1. Sign convention for rotations.

both simple and useful. Assumption 2 is to be substituted in the constitutive equation; ϵ_{33} is to be solved for and subsequently eliminated.

(c) Assumption (3) implies that plane sections remain plane. θ_α is interpreted as the rotation of a fiber, initially normal to the plate midsurface (i.e. $z = 0$).

The sign convention is illustrated in fig. 1. 'Right-hand rule' rotations $\hat{\theta}_\alpha$ are defined by $\theta_\alpha = -e_{\alpha\beta}\hat{\theta}_\beta$, where $e_{\alpha\beta}$ is the alternator tensor, namely

$$[e_{\alpha\beta}] = \begin{pmatrix} 0 & 1 \\ -1 & 0 \end{pmatrix}.$$ (10)

We prefer to develop the theory in terms of θ_α, rather than $\hat{\theta}_\alpha$, since the algebra is greatly simplified due to the absence of alternator tensors.

2.3. Constitutive equation

The reduced form of the constitutive equation used in the plate theory is determined by substituting assumption (2) into the three-dimensional constitutive equation and eliminating ϵ_{33}. For simplicity, we shall consider the isotropic case in which

$$t_{ij} = \lambda\delta_{ij}\epsilon_{kk} + 2\mu\epsilon_{ij},$$ (11)

where λ and μ are the Lamé coefficients and δ_{ij} is the Kronecker delta. Assumption (2) implies

$$\epsilon_{33} = \frac{-\lambda}{\lambda + 2\mu}\,\epsilon_{\alpha\alpha},$$ (12)

$$t_{\alpha\beta} = \bar{\lambda}\delta_{\alpha\beta}\epsilon_{\gamma\gamma} + 2\mu\epsilon_{\alpha\beta},$$ (13)

$$t_{\alpha3} = 2\mu\epsilon_{\alpha3},$$ (14)

where

$$\bar{\lambda} = 2\lambda\mu/(\lambda + 2\mu).$$ (15)

$\bar{\lambda}$ and μ may be eliminated in favor of E and ν (Young's modulus and Poisson's ratio, respectively):

$$\bar{\lambda} = \nu E/(1 - \nu^2),$$ (16)

$$\mu = E/[2(1 + \nu)].$$ (17)

2.4. Strain-displacement equations

Assumptions (3) and (4) lead to the following form of the strain-displacement equations:

$$\epsilon_{\alpha\beta} = u_{(\alpha,\beta)} = -z\theta_{(\alpha,\beta)},$$ (18)

$$\epsilon_{\alpha3} = u_{(\alpha,3)} = (-\theta_\alpha + w_{,\alpha})/2.$$ (19)

2.5. Summary of plate theory notations

w	transverse displacement,
θ_α	rotation vector,
$\kappa_{\alpha\beta} = \theta_{(\alpha,\beta)}$	curvature tensor,
$\gamma_\alpha = -\theta_\alpha + w_{,\alpha}$	shear strain vector,
$m_{\alpha\beta} = \displaystyle\int_{-t/2}^{t/2} t_{\alpha\beta}z\,\mathrm{d}z$	moment tensor,
$q_\alpha = \displaystyle\int_{-t/2}^{t/2} t_{\alpha3}\,\mathrm{d}z$	shear force vector,
W	prescribed boundary displacement
Θ_α	prescribed boundary rotations,
$F = \displaystyle\int_{-t/2}^{t/2} f_3\,\mathrm{d}z + \langle h_3\rangle$ *	total applied transverse force (per unit area),
$C_\alpha = \displaystyle\int_{-t/2}^{t/2} f_\alpha z\,\mathrm{d}z + \langle h_\alpha z\rangle$	total applied couple (per unit area),
$M_\alpha = \displaystyle\int_{-t/2}^{t/2} h_\alpha z\,\mathrm{d}z$	prescribed boundary moments,

* The operator $\langle\ \rangle$ is defined as follows: Let f be an arbitrary function of x, y and z. Then $\langle f(x, y, z)\rangle = f(x, y, -t/2) + f(x, y, t/2)$.

$$Q = \int_{-t/2}^{t/2} h_3 \, dz \qquad \text{prescribed boundary shear force.}$$

2.6. Variational equation

The variational equation of the plate theory is derived from the variational equation of the three-dimensional theory by making use of the preceding relations. The main steps are as follow.

(i) Let s_1 and s_2 be subregions of s which satisfy $\overline{s_1 \cup s_2} = s$ and $s_1 \cap s_2 = \emptyset$. The integrals appearing in the three-dimensional variational equations are replaced by the following iterated integrals:

$$\int_\Omega \ldots \, d\Omega = \int_A \int_{-t/2}^{t/2} \ldots \, dz \, dA, \qquad (20)$$

$$\int_{\Gamma_2} \ldots \, d\Gamma = \int_A \langle \ldots \rangle \, dA + \int_{s_2} \int_{-t/2}^{t/2} \ldots \, dz \, ds. \qquad (21)$$

The kinematic relations are also employed, yielding

$$0 = \int_A \int_{-t/2}^{t/2} [t_{\alpha\beta} \bar{u}_{(\alpha,\beta)} + 2 t_{\alpha 3} \bar{u}_{(\alpha,3)}] \, dz \, dA$$

$$- \int_A \int_{-t/2}^{t/2} (f_\alpha \bar{u}_\alpha + f_3 \bar{u}_3) \, dz \, dA$$

$$- \int_A (\langle h_\alpha \bar{u}_\alpha \rangle + \langle h_3 \bar{u}_3 \rangle) \, dA$$

$$- \int_{s_2} \int_{-t/2}^{t/2} (h_\alpha \bar{u}_\alpha + h_3 \bar{u}_3) \, dz \, ds$$

$$= \int_A \int_{-t/2}^{t/2} (-t_{\alpha\beta} z \bar{\kappa}_{\alpha\beta} + t_{\alpha 3} \bar{\gamma}_\alpha) \, dz \, dA$$

$$- \int_A \int_{-t/2}^{t/2} (-f_\alpha z \bar{\theta}_\alpha + f_3 \bar{w}) \, dz \, dA$$

$$- \int_A (-\langle h_\alpha z \rangle \bar{\theta}_\alpha + \langle h_3 \rangle \bar{w}) \, dA$$

$$- \int_{s_2} \int_{-t/2}^{t/2} (-h_\alpha z \bar{\theta}_\alpha + h_3 \bar{w}) \, dz \, ds, \qquad (22)$$

where

$$\bar{\kappa}_{\alpha\beta} = \bar{\theta}_{(\alpha,\beta)}, \qquad (23)$$

$$\bar{\gamma}_\alpha = -\bar{\theta}_\alpha + \bar{w}_{,\alpha}. \qquad (24)$$

(ii) The definitions of force resultants are used yielding

$$0 = \int_A (-m_{\alpha\beta} \bar{\kappa}_{\alpha\beta} + q_\alpha \bar{\gamma}_\alpha) \, dA$$

$$- \int_A (-C_\alpha \bar{\theta}_\alpha + F\bar{w}) \, dA - \int_{s_2} (-M_\alpha \bar{\theta}_\alpha + Q\bar{w}) \, ds. \qquad (25)$$

(iii) Integration by parts indicates, under the usual hypotheses, the differential equations and boundary conditions which are satisfied:

$$0 = \int_A \underbrace{(m_{\alpha\beta,\beta} - q_\alpha + C_\alpha)}_{\text{moment equil.}} \bar{\theta}_\alpha \, dA - \int_A \underbrace{(q_{\alpha,\alpha} + F)}_{\substack{\text{transverse} \\ \text{equil.}}} \bar{w} \, dA$$

$$+ \int_{s_2} \{ \underbrace{(-m_{\alpha n} + M_\alpha)}_{\text{moment b.c.}} \bar{\theta}_\alpha + \underbrace{(q_n - Q)}_{\text{shear b.c.}} \bar{w} \} \, ds, \qquad (26)$$

where

$$m_{\alpha n} = m_{\alpha\beta} n_\beta, \qquad (27)$$

$$q_n = q_\alpha n_\alpha. \qquad (28)$$

(iv) Explicit forms of the constitutive equations in terms of the plate-theory variables are computed as follows:

$$m_{\alpha\beta} = \int_{-t/2}^{t/2} t_{\alpha\beta} z \, dz$$

$$= \int_{-t/2}^{t/2} (\bar{\lambda} \delta_{\alpha\beta} \epsilon_{\gamma\gamma} + 2\mu \epsilon_{\alpha\beta}) z \, dz$$

$$= -\frac{t^3}{12} [\bar{\lambda} \delta_{\alpha\beta} \theta_{\gamma,\gamma} + 2\mu \theta_{(\alpha,\beta)}]$$

$$= -c_{\alpha\beta\gamma\delta} \kappa_{\gamma\delta}, \qquad (29)$$

where

$$c_{\alpha\beta\gamma\delta} = \frac{t^3}{12} \{ \mu (\delta_{\alpha\gamma} \delta_{\beta\delta} + \delta_{\alpha\delta} \delta_{\beta\gamma}) + \bar{\lambda} \delta_{\alpha\beta} \delta_{\gamma\delta} \}, \qquad (30)$$

$$q_\alpha = \int_{-t/2}^{t/2} t_{\alpha 3} \, dz$$

$$= \int_{-t/2}^{t/2} 2\mu\epsilon_{\alpha 3} \, \mathrm{d}z$$

$$= t\mu(-\theta_\alpha + w_{,\alpha})$$

$$= c_{\alpha\beta}\gamma_\beta , \tag{31}$$

$$c_{\alpha\beta} = t\mu\delta_{\alpha\beta}. \tag{32}$$

Remarks

(a) More general material behavior (e.g. orthotropy) can be considered by appropriately redefining the elastic coefficients $c_{\alpha\beta\gamma\delta}$ and $c_{\alpha\beta}$.

(b) Symmetry of the stiffness matrix will follow from the symmetries

$$c_{\alpha\beta\gamma\delta} = c_{\gamma\delta\alpha\beta}, \tag{33}$$

$$c_{\alpha\beta} = c_{\beta\alpha}. \tag{34}$$

The additional symmetries

$$c_{\alpha\beta\gamma\delta} = c_{\beta\alpha\gamma\delta} = c_{\alpha\beta\delta\gamma} \tag{35}$$

also hold.

(c) To achieve results consistent with classical bending theory it is necessary to introduce a 'shear correction factor' κ in the shear force–shear strain constitutive equation. This can be done by replacing $c_{\alpha\beta}$ by $\kappa c_{\alpha\beta}$. *Throughout we assume* $\kappa = \frac{5}{6}$.

2.7. Formal statement of the strong form of the plate theory boundary-value problem

Given F, C_α, M_α, Q, W and Θ_α, find w and θ_α such that

$$m_{\alpha\beta,\beta} - q_\alpha + C_\alpha = 0 \tag{36}$$

$$q_{\alpha,\alpha} + F = 0 \tag{37}$$

$$m_{\alpha\beta} = -c_{\alpha\beta\gamma\delta}\kappa_{\gamma\delta} \tag{38}$$

$$q_\alpha = c_{\alpha\beta}\gamma_\beta \tag{39}$$

$$\kappa_{\alpha\beta} = \theta_{(\alpha,\beta)} \tag{40}$$

$$\gamma_\alpha = -\theta_\alpha + w_{,\alpha}, \tag{41}$$

$\left.\right\}$, in A,

$$\theta_\alpha = \Theta_\alpha \tag{42}$$

$$w = W \tag{43}$$

$\left.\right\}$, on s_1,

$$m_{\alpha n} = m_{\alpha\beta}n_\beta = M_\alpha \tag{44}$$

$$q_n = q_\alpha n_\alpha = Q \tag{45}$$

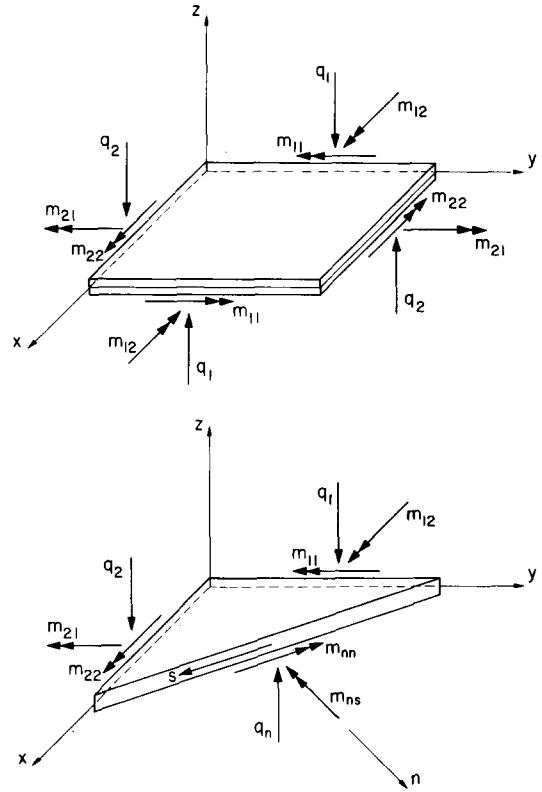$\left.\right\}$, on s_2.

Fig. 2. Sign convention for stress resultants.

Sign conventions for stress resultants are depicted in fig. 2.

2.8. Statement of the variational, or weak, form of the boundary-value problem

The spaces we will need are as follows:

$$L_2 = L_2(A) = \{v \mid v: A \to \mathcal{R}, \int_A v^2 \, \mathrm{d}A < \infty\}, \tag{46}$$

$$H^1 = H^1(A) = \{v \mid v \in L_2, v_{,\alpha} \in L_2\} \tag{47}$$

$$H^1_g = H^1_g(A) = \{v \mid v \in H^1, v(x,y) = g(x,y),$$

$$(x, y) \in s_1\} \tag{48}$$

(g will take on, in turn, the values W, Θ_α and 0).

Given F, C_α, M_α, Q, W and Θ_α, sufficiently regular, find $w \in H^1_W$ and $\theta_\alpha \in H^1_{\Theta_\alpha}$ such that, for all $\bar{w} \in H^1_0$

and $\bar{\theta}_\alpha \in H_0^1$

$$0 = \int_A [c_{\alpha\beta\gamma\delta}\,\theta_{(\gamma,\delta)}\bar{\theta}_{(\alpha,\beta)} + c_{\alpha\beta}\gamma_\beta\bar{\gamma}_\alpha]\,\mathrm{d}A$$

$$+ \int_A (C_\alpha\bar{\theta}_\alpha - F\bar{w})\,\mathrm{d}A + \int_{s_2} (M_\alpha\bar{\theta}_\alpha - Q\bar{w})\,\mathrm{d}s. \quad (49)$$

This can be written, in the usual way, as

$$\mathscr{A}(u, v) = (f, v) + (h, v)_\partial\,, \quad (50)$$

where

$$u = (\theta_1, \theta_2, w), \quad (51)$$

$$v = (\bar{\theta}_1, \bar{\theta}_2, \bar{w}), \quad (52)$$

$$f = (-C_1, -C_2, F), \quad (53)$$

$$h = (-M_1, -M_2, Q), \quad (54)$$

$$\mathscr{A}(u, v) = \int_A [c_{\alpha\beta\gamma\delta}\,\theta_{(\gamma,\delta)}\bar{\theta}_{(\alpha,\beta)} + c_{\alpha\beta}\gamma_\beta\bar{\gamma}_\alpha]\,\mathrm{d}A, \quad (55)$$

$$(f, v) = -\int_A (C_\alpha\bar{\theta}_\alpha - F\bar{w})\,\mathrm{d}A, \quad (56)$$

$$(h, v)_\partial = -\int_{s_2} (M_\alpha\theta_\alpha - Q\bar{w})\,\mathrm{d}s. \quad (57)$$

$\mathscr{A}(\cdot,\cdot)$ is symmetric and, for all appropriate boundary conditions, positive definite.

2.9. Matrix formulation of the variational equation

For computer programming purposes, it is convenient to employ a matrix formulation of the variational equation, given as follows:

$$0 = \int_A (\bar{\varkappa}^\mathrm{T} D^\mathrm{b}\varkappa + \bar{\gamma}^\mathrm{T} D^\mathrm{s}\gamma)\,\mathrm{d}A$$

$$+ \int_A (\bar{\theta}^\mathrm{T} C - \bar{w}F)\,\mathrm{d}A + \int_{s_2} (\bar{\theta}^\mathrm{T} M - \bar{w}Q)\,\mathrm{d}s, \quad (58)$$

where

$$\theta = \begin{Bmatrix} \theta_1 \\ \theta_2 \end{Bmatrix}; \qquad \bar{\theta} = \begin{Bmatrix} \bar{\theta}_1 \\ \bar{\theta}_2 \end{Bmatrix}, \quad (59)$$

$$\gamma = \begin{Bmatrix} \gamma_1 \\ \gamma_2 \end{Bmatrix}; \qquad \bar{\gamma} = \begin{Bmatrix} \bar{\gamma}_1 \\ \bar{\gamma}_2 \end{Bmatrix}, \quad (60)$$

$$\varkappa = \begin{Bmatrix} \kappa_{11} \\ \kappa_{22} \\ 2\kappa_{12} \end{Bmatrix}; \qquad \bar{\varkappa} = \begin{Bmatrix} \bar{\kappa}_{11} \\ \bar{\kappa}_{22} \\ 2\bar{\kappa}_{12} \end{Bmatrix}, \quad (61)$$

$$D^\mathrm{b} = \begin{bmatrix} D_{11}^\mathrm{b} & D_{12}^\mathrm{b} & D_{13}^\mathrm{b} \\ & D_{22}^\mathrm{b} & D_{23}^\mathrm{b} \\ \mathrm{symm.} & & D_{33}^\mathrm{b} \end{bmatrix}, \quad (62)$$

$$D_{IJ}^\mathrm{b} = c_{\alpha\beta\gamma\delta}, \quad (63)$$

in which

$$I/J = 1, 2, 3,$$

$$\alpha/\gamma = 1, 2, 1,$$

$$\beta/\delta = 1, 2, 2,$$

$$D^\mathrm{s} = \begin{pmatrix} D_{11}^\mathrm{s} & D_{12}^\mathrm{s} \\ \mathrm{symm.} & D_{22}^\mathrm{s} \end{pmatrix}, \quad (64)$$

$$D_{\alpha\beta}^\mathrm{s} = c_{\alpha\beta}. \quad (65)$$

2.10. Finite element stiffness matrix and load vector

The finite element stiffness matrix and load vector may be obtained directly from the matrix form of the variational equation. The finite element approximations of w, $\bar{w}$, θ_α and $\bar{\theta}_\alpha$ are denoted w^h, $\bar{w}^h$, θ_α^h and $\bar{\theta}_\alpha^h$, respectively. In a typical element, possessing N_{en} nodes,

$$w^h = \sum_{a=1}^{N_{en}} N_a w_a^h, \quad (66)$$

$$\bar{w}^h = \sum_{a=1}^{N_{en}} N_a \bar{w}_a^h, \quad (67)$$

$$\theta_\alpha^h = \sum_{a=1}^{N_{en}} N_a \theta_{\alpha a}^h, \quad (68)$$

$$\bar{\theta}_\alpha^h = \sum_{a=1}^{N_{en}} N_a \bar{\theta}_{\alpha a}^h, \quad (69)$$

where N_a is the shape function associated with node a, and w_a^h, $\bar{w}_a^h$, $\theta_{\alpha a}^h$ and $\bar{\theta}_{\alpha a}^h$ are the ath nodal values of w^h, $\bar{w}^h$, θ_α^h and $\bar{\theta}_\alpha^h$, respectively.

Remark

It is not necessary to assume θ_α^h and w^h are defined in terms of the same shape functions and nodal patterns. However, in the applications we have in mind, this will be the case.

Define

$$d = \{d_I\}; \qquad \bar{d} = \{\bar{d}_I\}, \qquad (70, 71)$$

$$d_I = \begin{cases} w_a^h, & I = 3a - 2, \\ \theta_{1a}^h, & \cdot \ I = 3a - 1, \\ \theta_{2a}^h, & I = 3a, \end{cases} \qquad (72)$$

$$\bar{d}_I = \begin{cases} \bar{w}_a^h, & I = 3a - 2, \\ \bar{\theta}_{1a}^h, & I = 3a - 1, \\ \bar{\theta}_{2a}^h, & I = 3a, \end{cases} \qquad (73)$$

$$\varkappa = B^b d; \qquad \bar{\varkappa} = B^b \bar{d}, \qquad (74)$$

$$\gamma = B^s d; \qquad \bar{\gamma} = B^s \bar{d}, \qquad (75)$$

$$B^b = [B_1^b, B_2^b, ..., B_{N_{en}}^b], \qquad (76)$$

$$B^s = [B_1^s, B_2^s, ..., B_{N_{en}}^s], \qquad (77)$$

$$B_a^b = \begin{bmatrix} 0 & N_{a,x} & 0 \\ 0 & 0 & N_{a,y} \\ 0 & N_{a,y} & N_{a,x} \end{bmatrix}, \qquad (78)$$

$$B_a^s = \begin{pmatrix} N_{a,x} & -N_a & 0 \\ N_{a,y} & 0 & -N_a \end{pmatrix}. \qquad (79)$$

With these definitions the following expressions for the element stiffness and load may be obtained:

$$k^e = k_b^e + k_s^e, \qquad (80)$$

$$k_b^e = \int_{A^e} B^{bT} D^b B^b \, dA, \qquad \text{bending stiffness,} \qquad (82)$$

$$k_s^e = \int_{A^e} B^{sT} D^s B^s \, dA, \qquad \text{shear stiffness,} \qquad (82)$$

$$f^e = \{f_I^e\} \qquad (83)$$

$$f_I^e = \begin{cases} \int_{A^e} N_a F \, dA + \int_{s^e \cap s_2} N_a Q \, ds, & I = 3a - 2, \\ -\int_{A^e} N_a C_1 \, dA - \int_{s^e \cap s_2} N_a M_1 \, ds, & \\ & I = 3a - 1, \\ -\int_{A^e} N_a C_2 \, dA - \int_{s^e \cap s_2} N_a M_2 \, ds, & \\ & I = 3a, \end{cases} \qquad (84)$$

where A^e and s^e are the area and boundary, respectively, of the *e*th element.

The adjustment to f_I^e for prescribed displacements is given by

$$f_I^e \leftarrow f_I^e - \sum_{J=1}^{N_{ee}} k_{JI}^e g_J, \qquad N_{ee} = 3N_{en}, \qquad (85)$$

where

$$g_I = \begin{cases} W(x_a, y_a), & I = 3a - 2, \\ \Theta_1(x_a, y_a), & I = 3a - 1, \\ \Theta_2(x_a, y_a), & I = 3a. \end{cases} \qquad (86)$$

3. Plate bending finite elements

A salient feature of the present theory is that, at most, only first derivatives of w and θ_α appear in the variational equations. *The practical consequence of this fact is that only C^0 continuous finite element functions need be employed.* This is to be contrasted with the classical thin plate theory, in which second derivatives appear in the variational equations, necessitating the use of C^1 continuous finite element functions. One may safely assert that it is this latter condition, so difficult to achieve in practice, which has precluded the development of simple and effective 'displacement' elements. On the other hand, C^0 continuity may be achieved by any number of finite element interpolatory schemes, a key advantage of the present theory.

3.1. Shear constraints and 'locking'

An important consideration in the development of plate bending elements, based upon the present theory, is the number of shear strain constraints

engendered in the thin plate limit (i.e. as $t \to 0$). To see this, we consider a heuristic example.

Example

Assume a four-node isoparametric quadrilateral element and, for simplicity, assume the element is of rectangular plan and the sides are aligned with the global x and y axes. In this case the element expansions may be written as

$$w^h = \beta_0 + \beta_1 x + \beta_2 y + \beta_3 xy, \tag{87}$$

$$\theta_\alpha^h = \gamma_{\alpha 0} + \gamma_{\alpha 1} x + \gamma_{\alpha 2} y + \gamma_{\alpha 3} xy, \tag{88}$$

where β_i and $\gamma_{\alpha i}$, $0 \leqslant i \leqslant 3$, are constants which depend upon the nodal parameters w_a^h and $\theta_{\alpha a}^h$, $1 \leqslant a \leqslant 4$, respectively. The conditions

$$0 = \gamma_1$$

$$= -\theta_1^h + w_{,1}^h$$

$$= (\gamma_{10} + \beta_1) - \gamma_{11} x + (-\gamma_{12} + \beta_3) y - \gamma_{13} xy, \tag{89}$$

$$0 = \gamma_2$$

$$= -\theta_2^h + w_{,2}^h$$

$$= (-\gamma_{20} + \beta_2) + (-\gamma_{21} + \beta_3) x - \gamma_{22} y - \gamma_{23} xy, \tag{90}$$

impose eight constraints per element, and are approximately in force as $t \to 0$, if exact integration of k_s^e is performed. (Two-by-two Gauss integration is exact in this case.) In a large rectangular mesh there are approximately three degrees of freedom per element, and thus the element tends to be overly constrained. In practice, worthless numerical results are obtained (see Pugh [2]). To alleviate the 'locking' effect, one might consider using one-point Gauss quadrature for k_s^e. Clearly, this results in only two constraints per element, and now there are more degrees of freedom than there are constraints. This element, with one-point shear integration and two-by-two bending integration, was proposed, and shown to be successful, by Hughes et al. [3].

. Arguments, similar to those in the above example, have been used to evaluate other possibilities (see Pugh et al. [2,4] and Malkus and Hughes [5]). *The main conclusion to be drawn is that the Lagrange family of isoparametric quadrilaterals, with appropriate reduced integration on the shear term, is the most promising of the standard element families.*

Numerical data in support of this conclusion are contained in Pugh [2], who has shown that triangles

and serendipity quadrilateral elements are, at best, less accurate than Lagrange elements and, at worst, divergent in the thin plate limit. Based on these facts, we will, in the remainder of this paper, concern ourselves only with the most important elements in the Lagrange family.

3.2. Reduced integration Lagrange plate elements

To avoid shear 'locking' in thin plates, some form of reduced integration must be employed. Two concepts have been used with success: *uniform reduced integration* and *selective reduced integration.*

In uniform reduced integration both the bending and shear terms are integrated with the same rule, which is of lower order than the 'normal' one. Apparently, the first example of a uniform reduced integration plate element was the eight-node serendipity element of Zienkiewicz et al. [6], in which two-by-two Gauss quadrature was employed. Although this element has received wide use, it has just recently been shown to behave poorly in the thin plate limit [2,4]. Nevertheless, reduced integration still represents a considerable improvement over normal integration.

In selective reduced integration the bending term is integrated with the 'normal' rule, whereas the shear term is integrated with a lower-order rule.

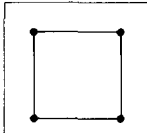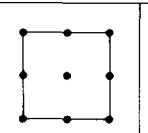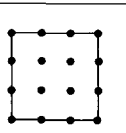Integration rules for Lagrange plate bending elements are indicated in fig. 3. Numerical results for S1

w, θ_1, θ_2 shape functions	bilinear	biquadratic	bicubic
Uniform reduced integration	1 × 1 U 1	2 × 2 U 2	3 × 3 U 3
Selective reduced integration	1 × 1 shear 2 × 2 bending S 1	2 × 2 shear 3 × 3 bending S 2	3 × 3 shear 4 × 4 bending S 3

Fig. 3. Lagrange plate elements. Three degrees-of-freedom per node: w, θ_1, θ_2.

have been presented by Hughes et al. [3] and Pugh et al. [2,4], and results for U2 and U3 have also been presented by Pugh et al. [2,4]. In this paper, results are presented for U1, U2, S1 and S2. (Apparently S3 has yet to be studied.)

As $t \to 0$, the shear strains at the Gauss points of the shear quadrature rule approach zero. Thus, in the thin plate limit the present elements may be viewed as 'discrete Kirchhoff elements'. The superior behavior of reduced integration Lagrange elements in handling extremely thin plates has been exhibited in [2–4].

3.3. Selective integration and invariance

Selective reduced integration was first employed by Doherty et al. [7] on a four-node elasticity element to improve its bending behavior. Although improved results were noted in certain configurations, a lack of invariance with respect to coordinate transformations caused the element to be abandoned. Due to a potential lack of invariance, we have been admonished against selective integration by Kavanagh and Key [8]. However, we wish to point out that lack of invariance is not a necessary by-product of the use of selective integration, but a consequence of its misuse. To illustrate this we shall present a simple test which guarantees invariance when selective integration is used. First, we wish to make precise what we mean by 'invariance with respect to coordinate transformation'. The coordinate transformations we have in mind are changes of the global reference frame. For simplicity we shall consider only rectangular cartesian reference frames. (The results actually hold in the fully general case of arbitrary curvilinear systems.) Let (x_1, x_2, x_3) and (x'_1, x'_2, x'_3) be coordinate functions for two such frames of reference. Vector fields transform as

$$u'_i = Q_{ij} u_j, \tag{91}$$

where u_i and u'_i are components in the unprimed and primed systems, respectively, and Q_{ij} is orthogonal (i.e. $Q_{ik} Q_{jk} = \delta_{ij}$). An example of a quantity 'invariant with respect to coordinate transformations' is the dot product:

$$u'_i u'_i = u_i u_i. \tag{92}$$

An example of a non-invariant quantity is u_1, since in general
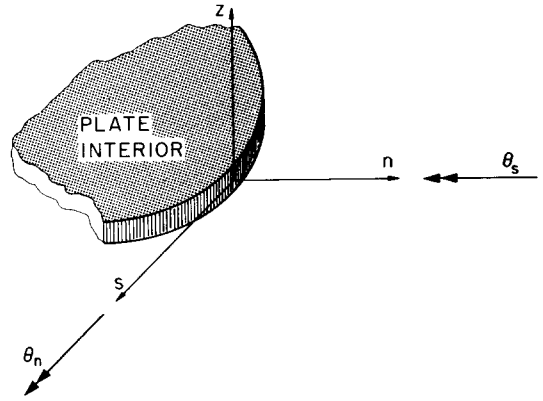
$$u'_1 \neq u_1. \tag{93}$$

Fig. 4. Local tangential–normal coordinate system at plate boundary.

Now suppose we wish numerically to integrate a function f over some domain $\square$ in $\mathcal{R}^n$ (e.g. think of $\square$ as the biunit square in $\mathcal{R}^2$). Suppose

$$f = g + h \tag{94}$$

and let the quadrature formula be given by

$$\int_{\square} f \, d\square \cong \sum_{i=1}^{N_{\text{int}}^{(1)}} g(\tilde{\xi}_i^{(1)}) W_i^{(1)} + \sum_{i=1}^{N_{\text{int}}^{(2)}} h(\tilde{\xi}_i^{(2)}) W_i^{(2)}, \tag{95}$$

where $N_{\text{int}}^{(\alpha)}$, $\{\tilde{\xi}_i^{(\alpha)}\}$ and $\{W_i^{(\alpha)}\}$ are the number of integration points, the locations and the weights, respectively, of the αth rule. We assume the locations are defined in an invariant manner with respect to $\square$. *Then, if g and h are each invariant with respect to coordinate transformations, the right-hand side of (95) is invariant.*

The selective integration elements described herein are invariant, since the bending and shear energy densities (i.e. g and h, respectively) are invariants.

Note that, for the element of Doherty et al. [7], neither g nor h is invariant, in violation of the above requirement.

3.4. Boundary conditions

It is important to realize that boundary conditions in the present theory are not always the same as those for the classical thin plate theory. The differences occur in the specification of the 'simply supported' case. In the present theory there are two ways of going about this, depending on the actual physical constraint.
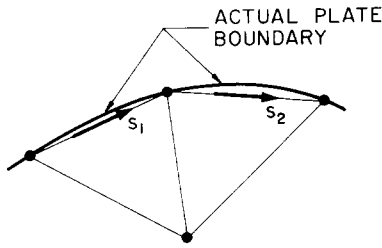
Fig. 5. Approximation to curved plate boundary by straight-edged finite elements.

Rather than being an additional complication, this freedom turns out to be a considerable benefit, for it enables the solution of problems in which thin plate finite elements have heretofore failed (see Rossow [9] and Scott [10]).

Consider a smooth portion of the plate boundary and a local s, n coordinate system to it. (s denotes the tangential direction and n the outward normal direction; see fig. 4.) The most common boundary conditions encountered in practice are given as follows:

clamped:

$w = 0$; $\theta_s = 0$; $\theta_n = 0$,

free:

$Q = 0$; $M_s = 0$; $M_n = 0$,

simply supported:

SS_1 $w = 0$; $M_s = 0$; $M_n = 0$,

SS_2 $w = 0$; $\theta_s = 0$; $M_n = 0$,

symmetric:

$Q = 0$; $M_s = 0$; $\theta_n = 0$,

skew symmetric: *

$w = 0$; $\theta_s = 0$; $M_n = 0$.

In thin plate theory, SS_2 is the appropriate simply-supported boundary condition, since $w = 0$ along the boundary necessitates $\partial w/\partial s = 0$, and the absence of shear strains requires $\theta_s = \partial w/\partial s$. When curved-boundary, simply-supported plates are approximated by

* Observe that SS_2 and the skew-symmetric case are the same.

straight-edged, thin plate elements, SS_2 leads to difficulties. For in this case, specifying $\partial w/\partial s = 0$ at interelement boundaries, for which s is not collinear (see fig. 5), implies $\partial w/\partial n = 0$ as well. Thus, as the mesh is refined, the clamped boundary condition is achieved. In other words, the correct solution to the *wrong* problem is attained! Strategies for circumventing this 'paradox' tend to be inconvenient from an implementational standpoint (for further details see Scott [10]).

Another 'paradox', discussed by Rossow [9], concerns the solution of a uniformly loaded, simply-supported, rhombic thin plate. The analytic solution is singular in the vicinity of the obtuse vertices, with moments of *opposite sign*. However, Sander [11] has reported solutions in which thin plate elements yield moments of the *same* sign. This phenomenon may also be traced to an overconstraining of thin plate elements caused by SS_2.

A pleasant feature of the present theory is that the alternative, simply-supported boundary condition, SS_1, completely obviates these 'paradoxes'. In cases in which there is no danger of overconstraining, such as simply-supported rectangular plates, SS_2 may be employed to further eliminate degrees of freedom, for greater economy of solution. Computations in support of these assertions are presented in section 5.

3.5. Equivalence with mixed methods

The plate elements discussed in this paper have been shown to be identical to elements derived from a mixed formulation, in which the shear forces, q_α, are variables in addition to w and θ_α; see Malkus and Hughes [5]. The shear variables, with nodes at the Gauss points of the shear integration rules, are discontinuous between elements. Some examples of equivalent elements are given below.

Examples

(1) Let w and θ_α be approximated by bilinear shape functions and let q_α take on constant values within each element. If one-point Gauss quadrature is used to construct the stiffness, it is equivalent to U1. If two-by-two Gauss quadrature is used on the bending term, and one-point Gauss quadrature is used on the remaining shear term, then the element is equivalent to S1. In each case, the constant value of q_α in the mixed formulation is the same as that computed
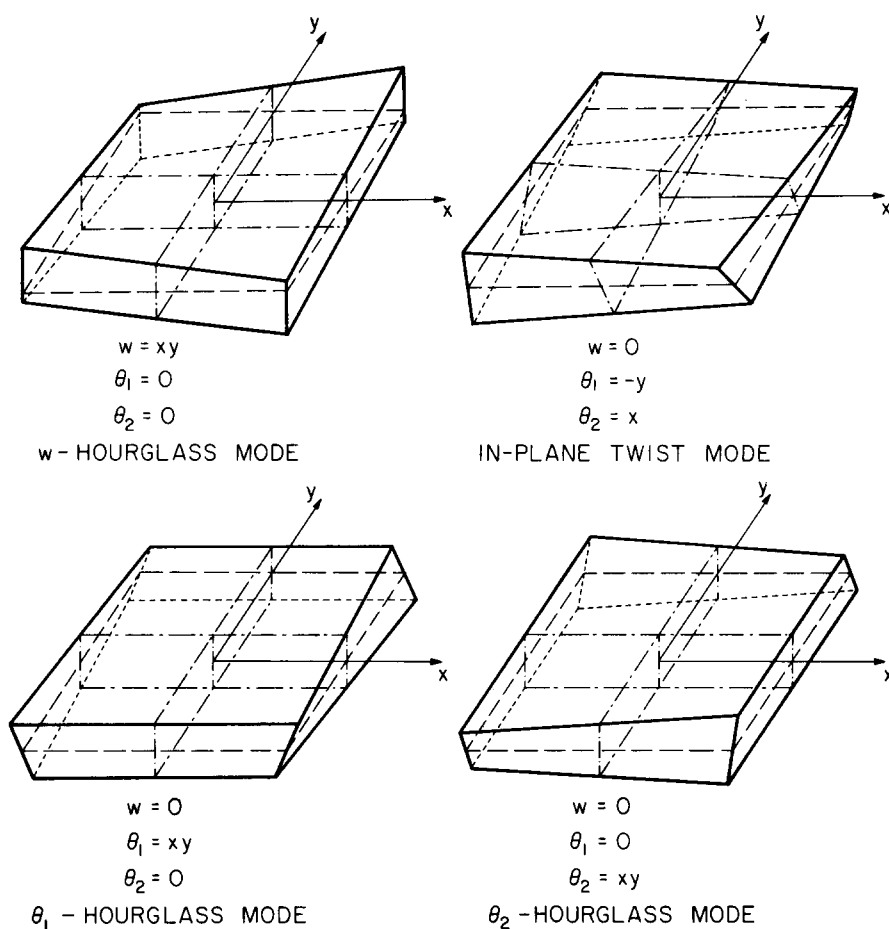
w = xy
$\theta_1 = 0$
$\theta_2 = 0$
w – HOURGLASS MODE

w = O
$\theta_1 = -y$
$\theta_2 = x$
IN-PLANE TWIST MODE

w = O
$\theta_1 = xy$
$\theta_2 = 0$
θ_1 – HOURGLASS MODE

w = O
$\theta_1 = 0$
$\theta_2 = xy$
θ_2 – HOURGLASS MODE

Fig. 6. Zero-energy modes of element U1.

from w and θ_α at the centroid of U1, or S1, respectively.

(2) Let w and θ_α be approximated by biquadratic shape functions and let q_α be approximated by bilinear shape functions. The nodes for q_α are the two-by-two Gauss points. If the two-by-two Gauss rule is used for all terms, the element is equivalent to U2. If the three-by-three rule is used on the bending term, and the two-by-two rule is used on the shear terms, the element is equivalent to S2. In each case, the bilinear variation of q_α within each element in the mixed formulation may be recaptured in U2 and S2, respectively, by passing a bilinear function through the two-by-two Gauss point values of q_α computed from w and θ_α.

Additional details on these and related matters may be found in Malkus and Hughes [5].

3.6. Rank deficiency

Perhaps the only negative feature of the reduced integration Lagrange plate elements is rank deficiency. This does not appear to be a hindrance in practical problem solving. On occasion, however, precautions need to be taken. The number of zero-energy modes possessed by each element, in excess of the three rigid-body modes, is presented in table 1. As can be clearly seen, the number is lower for each selective reduced integration element than for the corresponding uniform reduced integration element, an advantage of the former.

The four zero-energy modes of U1 are depicted in fig. 6. Element S1 possesses only the w hourglass and the in-plane twist mode.

The zero-energy modes for U2 are:

Table 1
Zero-energy modes, in excess of rigid-body modes, for
reduced integration, Lagrange, plate elements

Element	U1	U2	U3	S1	S2	S3
Number of zero-energy modes	4	4	4 *	2	1	?

* From Pugh et al. [4].

$$w = x^2 y^2 - \tfrac{1}{3}(x^2 + y^2), \quad \theta_1 = \theta_2 = 0, \tag{96}$$

$$w = 0, \quad \theta_1 = 0, \quad \theta_2 = (x^2 - \tfrac{1}{3})(y^2 - \tfrac{1}{3}), \tag{97}$$

$$w = 0, \quad \theta_1 = (x^2 - \tfrac{1}{3})(y^2 - \tfrac{1}{3}), \quad \theta_2 = 0, \tag{98}$$

$$w = 0, \quad \theta_1 = x(y^2 - \tfrac{1}{3}), \quad \theta_2 = -y(x^2 - \tfrac{1}{3}). \tag{99}$$

Only eq. (96) is present in S2.

In general, boundary conditions render the assembled stiffness matrix positive definite, and so the zero-energy modes are not globally present. A guideline which we have so far successfully employed for selective integration elements is: if the boundary conditions preclude the rigid mode from forming in one element, it is also precluded in the remainder of the mesh. It turns out that a sufficient condition for satisfying the guideline, for elements S1 and S2, is that two adjacent nodal values of w be specified in at least one element.

A critical test is provided by a point-supported, pergola roof *. The roof is assumed to be a square plate, subjected to uniform transverse load, and 'fixed' at the center. A mesh of square S1 elements was constructed with the center node clamped (i.e. $w = \theta_1 = \theta_2 = 0$). Rank check analyses have revealed that the in-plane twist mode disappears in a mesh of two or more S1 elements, so it is not a problem. However, the w hourglass is present unless eliminated via boundary conditions. As is clear, a global pattern, in which each element hourglasses, is possible in the present situation, since only one w degree of freedom is specified. (A rank check analysis confirmed this to be the case, indicating one zero mode.) An alternative mesh was employed in which the point support was distributed in a diamond pattern; see fig. 7. (In fact, this is more in keeping with the physical situation.) Since $w = 0$ along an edge of each of the four central

* We thank P.C. Jennings for suggesting this problem to us.
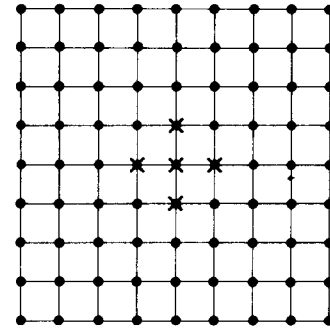
✕   denotes nodes at which $w = 0$

Fig. 7. Pergola roof. Mesh of S1 elements exhibiting no zero-energy modes

elements, these elements cannot hourglass. A rank check analysis revealed a positive-definite stiffness, in confirmation of this. Note that it is crucial to have $w = 0$ at the center, otherwise the w hourglass reappears.

A further study will have to be undertaken to assess the effects of the additional rank deficiency of the unifrom reduced integration elements. Some disappointing numerical results have been obtained for U1; see section 5.3.

3.7. Further convergence conditions

It is important to realize that convergence criteria for elements derived from the present theory are quite different to those for elements derived from thin plate theory. Necessary conditions in the present case are:

(1) all three rigid body modes must be exactly representable; and

(2) the following five constant strain states must be exactly representable:

$$\left. \begin{array}{l} \theta_{1,1} \\ \theta_{2,2} \\ \tfrac{1}{2}(\theta_{1,2} + \theta_{2,1}) \end{array} \right\} \text{'curvatures',}$$

$$\left. \begin{array}{l} \theta_1 - w_{,1} \\ \theta_2 - w_{,2} \end{array} \right\} \text{transverse shear strains.}$$

In complicated situations the above conditions may be verified by use of Irons' 'patch test' (see Strang

and Fix [12] for an exposition). It is easily verified that these conditions are satisfied for standard isoparametric elements, and for the reduced integration isoparametric elements described herein.

4. Transient analysis

The static theory of section 2 may be generalized to dynamics by the addition of inertial terms and the specification of initial conditions. We content ourselves here just with indicating the main steps involved in adding the inertial terms, and with pointing out some interesting properties of mass matrices derived from them. A superposed dot is used to denote time differentiation.

4.1. Mass matrices

The starting point is eq. (6), to which we add

$$\int_\Omega \rho \ddot{u}_i \bar{u}_i \, d\Omega \tag{100}$$

to the left-hand side, where ρ denotes the mass density. We assume for simplicity $\rho = \rho(x, y)$. Employing the assumptions and results of section 2 leads to the definition of the element mass matrix

$$m^e = [m^e_{IJ}], \tag{101}$$

$$m^e_{IJ} = \begin{cases} t m^e_{ab}, & I = 3a - 2, \quad J = 3b - 2, \\ \dfrac{t^3}{12} m^e_{ab}, & I = 3a - 1, \quad J = 3b - 1, \\ \dfrac{t^3}{12} m^e_{ab}, & I = 3a, \quad J = 3b, \end{cases} \tag{102}$$

$$m^e_{ab} = \int_{A^e} \rho N_a N_b \, dA. \tag{103}$$

Accurate Gauss quadrature of (103) yields coupled, 'consistent' mass matrices. A more computationally attractive scheme for Lagrange elements is provided by Lobatto quadrature, in which the nodal points coincide with the integration points. When applied to (103), *diagonal, positive-definite mass matrices are produced.* The first two one-dimensional, Lobatto rules are the trapezoidal rule and Simpson's rule. The evaluation points of the two-dimensional generaliza-

tions are the nodes of the four- and nine-node Lagrange elements, respectively. For the sixteen-node element, and higher-order elements, the nodes must be relocated at the 'Lobatto points'; see Fried and Malkus [13].

4.2. Critical time steps

In principle the construction of 'lumped' mass matrices by Lobatto rules opens the way to explicit transient calculations [4]. However, as we shall see, the time step restriction is stringent, suggesting an alternative definition of the mass matrix. To develop these ideas in the simplest possible setting, we shall employ a one-dimensional model, the linear beam [3], which exhibits all of the pertinent features.

In the linear beam element both w and θ are assumed to vary linearly over each element. One-point Gauss quadrature exactly integrates the bending stiffness and appropriately underintegrates the shear stiffness to avoid locking [3]. We assume the trapezoidal rule is used to develop the lumped mass matrix. The matrices for a typical element describing bending in the plane are:

$$k_b = \frac{EI}{h} \begin{bmatrix} 0 & 0 & 0 & 0 \\ 0 & 1 & 0 & -1 \\ 0 & 0 & 0 & 0 \\ 0 & -1 & 0 & 1 \end{bmatrix}, \tag{104}$$

$$k_s = \frac{\mu \hat{A}_s}{h} \begin{bmatrix} 1 & \frac{1}{2}h & -1 & \frac{1}{2}h \\ \frac{1}{2}h & \frac{1}{4}h^2 & -\frac{1}{2}h & \frac{1}{4}h^2 \\ -1 & -\frac{1}{2}h & 1 & -\frac{1}{2}h \\ \frac{1}{2}h & \frac{1}{4}h^2 & -\frac{1}{2}h & \frac{1}{4}h^2 \end{bmatrix}, \tag{105}$$

$$m = \rho \hat{A} \tfrac{1}{2} h \begin{bmatrix} 1 & 0 & 0 & 0 \\ 0 & I/\hat{A} & 0 & 0 \\ 0 & 0 & 1 & 0 \\ 0 & 0 & 0 & I/\hat{A} \end{bmatrix}, \tag{106}$$

where $\hat{A}$ is the cross-section area, $\hat{A}_s$ is the shear area, I is the moment of inertia, and h is the element length. We have assumed E, μ, $\hat{A}$, $\hat{A}_s$, I and ρ are constants within the element for simplicity. The degree-of-freedom ordering is $w_1, \theta_1, w_2, \theta_2$, where the subscript is the node number.

For a conditionally stable transient integrator, such as 'central differences', the critical time step, Δt_{crit}, must satisfy

$$\Delta t_{crit} \leq \text{const.}/\omega_{max}, \tag{107}$$

where ω_{max} is the maximum frequency of the system. In the case of the central difference operator, the constant in (107) is 2. It is a simple exercise to show that

$$\omega_{max} \leq \max_e (\omega_{max}^e), \tag{108}$$

where ω_{max}^e is the maximum frequency of the eth element, unrestrained.

Solution of the eigenvalue problem for the linear beam element yields the results shown in table 2, where $c^2 = E/\rho$, the bar-wave velocity, and $c_s^2 = \mu \hat{A}_s/(\rho \hat{A})$, the beam shear-wave velocity. The maximum frequency is given by

$$\omega_{max} = \max \left\{ \frac{2c}{h}, \left(\frac{2c_s}{h}\right)\left[1 + \frac{\hat{A}}{I}\left(\frac{h}{2}\right)^2\right]^{1/2} \right\}. \tag{109}$$

Thus, the critical time step for the central difference operator is given by

$$\Delta t_{crit} = \min \left\{ \frac{h}{c}, \left(\frac{h}{c_s}\right)\left[1 + \frac{\hat{A}}{I}\left(\frac{h}{2}\right)^2\right]^{-1/2} \right\}. \tag{110}$$

To get a feel for these quantities, we shall take a typical situation. Assume the cross-section is rectangular with depth t and width 1. This results in $\hat{A} = t$ and $I = t^3/12$. We assume the ratio of wave speeds $c/c_s = \sqrt{3}$. This corresponds to a Poisson's ratio of $\frac{1}{4}$ and shear correction factor $\kappa = \hat{A}_s/\hat{A} = \frac{5}{6}$, so it is a reasonable approximation for most metals. The time step incurred by the bending mode will be critical when

$$h/t \leq \sqrt{\tfrac{2}{3}} \cong 0.8165. \tag{111}$$

This would only be the case for a very deep beam or

an extremely fine mesh and is thus unlikely in practice The more typical situation in structural analysis is when $t \ll h$ (i.e. very thin beams or coarse meshing). In this case the critical time step is slightly less than t/c, the time for a bar wave to traverse the thickness. As this is an extremely small time step, the cost of explicit integration becomes prohibitive.

A more favorable condition can be derived by adopting different values for the rotational lumped mass coefficients. Specifically, we take

$$m = \rho \hat{A} \tfrac{1}{2} h \begin{bmatrix} 1 & 0 & 0 & 0 \\ 0 & \alpha & 0 & 0 \\ 0 & 0 & 1 & 0 \\ 0 & 0 & 0 & \alpha \end{bmatrix} \tag{112}$$

and select α to achieve a more desirable critical time step, without upsetting convergence. Beam mass matrices of the above type were introduced by Key and Beisinger [14]. This time, solution of the eigenvalue problem yields the values shown in table 3.

Table 2

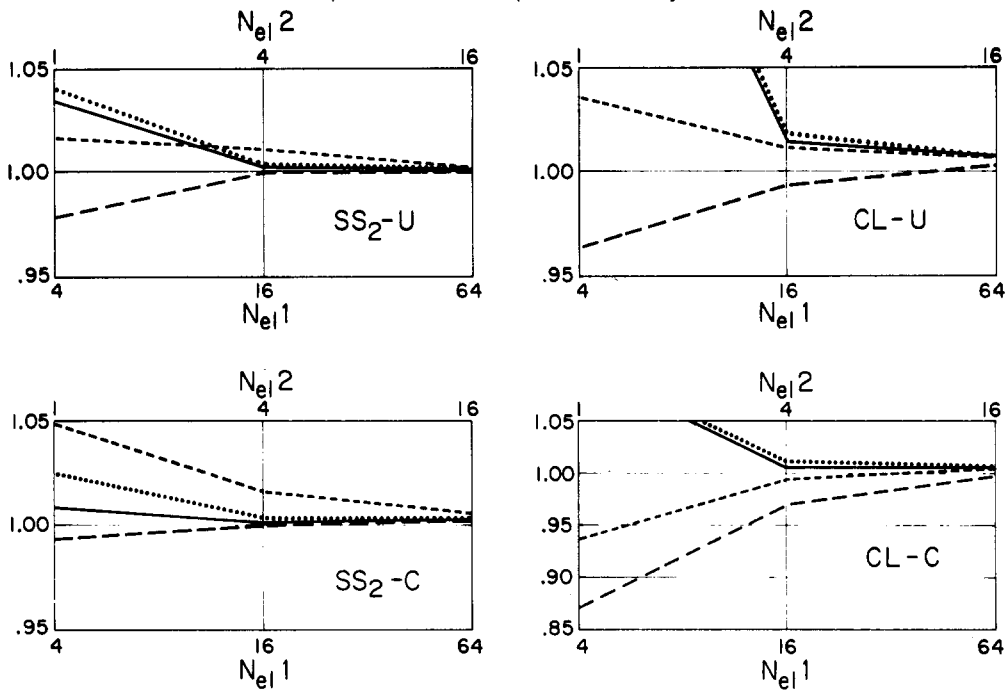| Eigenvalue	Eigenvector	Description
0	$(1\ 0\ 1\ 0)^T$	rigid translation
0	$\left(-1\ \dfrac{2}{h}\ 1\ \dfrac{2}{h}\right)^T$	rigid rotation
$4c^2/h^2$	$(0\ 1\ 0\ -1)^T$	bending
$\left(\dfrac{4c_s^2}{h^2}\right)\left[1 + \dfrac{\hat{A}}{I}\left(\dfrac{h}{2}\right)^2\right]$	$\left(1\ \dfrac{\hat{A}}{I}\dfrac{h}{2}\ -1\ \dfrac{\hat{A}}{I}\dfrac{h}{2}\right)^T$	shear

Table 3

Eigenvalue	Eigenvector	Description
0	$(1\ 0\ 1\ 0)^T$	rigid translation
0	$\left(-1\ \dfrac{2}{h}\ 1\ \dfrac{2}{h}\right)^T$	rigid rotation
$(4c^2/h^2)(I/\alpha\hat{A})$	$(0\ 1\ 0\ -1)^T$	bending
$\left(\dfrac{4c_s^2}{h^2}\right)\left[1 + \dfrac{1}{\alpha}\left(\dfrac{h}{2}\right)^2\right]$	$\left(1\ \dfrac{h}{2\alpha}\ -1\ \dfrac{h}{2\alpha}\right)^T$	shear
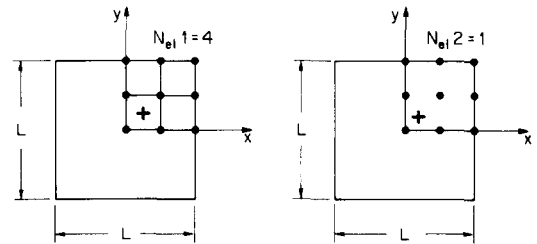
$N_{el}1$ - number of 4-node elements $N_{el}2$ - number of 9-node elements

+ denotes location of Gauss point nearest center
  (1×1 rule for 4-node elements and 2×2 rule for 9-node elements)

Fig. 8. Square plate. Due to symmetry, only one quadrant is discretized.

Center displacement normalized with
respect to thin plate theory

Moment at Gauss point nearest center,
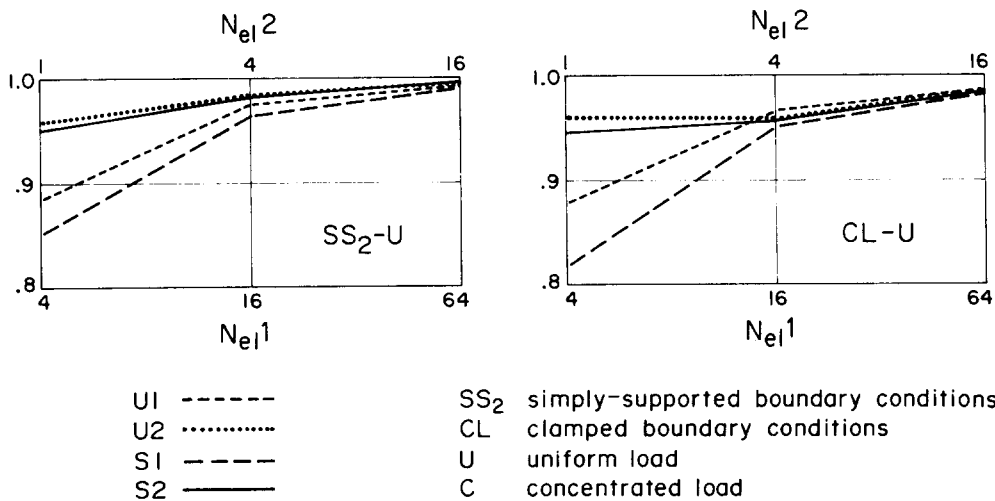normalized by center moment of thin
plate theory

UI	- - - - - -	SS₂	simply-supported boundary conditions
U2	⋯⋯⋯	CL	clamped boundary conditions
S I	— — — —	U	uniform load
S2	————	C	concentrated load

Fig. 9. Convergence study for thin quare plate.

+ denotes location of Gauss point nearest center.
(1×1 rule for 4-node elements and 2×2 rule for 9-node elements)
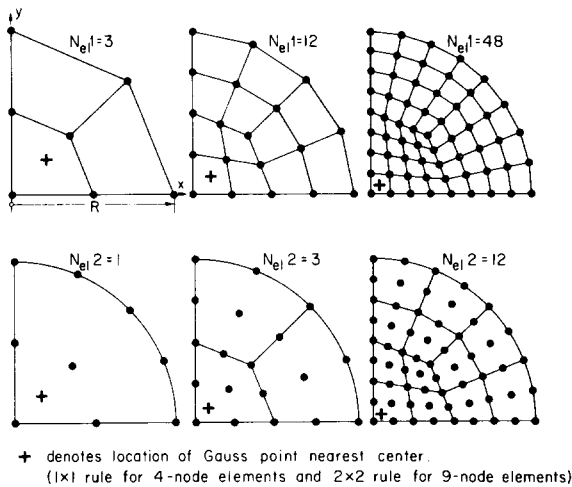
Fig. 10. Circular plate. Due to symmetry, only one quadrant is discretized.

The counterparts of eqs. (109) and (110) are, respectively,

$$\omega_{max} = \max \left\{ \left(\frac{2c}{h}\right)\left(\frac{I}{\alpha \hat{A}}\right)^{1/2}, \left(\frac{2c_s}{h}\right)\left[1 + \frac{1}{\alpha}\left(\frac{h}{2}\right)^2\right]^{1/2} \right\}.$$

(113)

$$\Delta t_{crit} = \min \left\{ \left(\frac{h}{c}\right)\left(\frac{\alpha \hat{A}}{I}\right)^{1/2}, \left(\frac{h}{c_s}\right)\left[1 + \frac{1}{\alpha}\left(\frac{h}{2}\right)^2\right]^{-1/2} \right\}.$$

(114)

Taking the value $\alpha = h^2/8$ in (114), and again assuming $\hat{A}/I = 12/t^2$ and $c/c_s = \sqrt{3}$, results in

$$\Delta t_{crit} = \min \left\{ \left(\frac{h}{c}\right)\left(\sqrt{\tfrac{3}{2}} \frac{h}{t}\right), \frac{h}{c} \right\}.$$

(115)

As long as

$$h/t > \sqrt{\tfrac{2}{3}} \cong 0.8165$$

(116)

we achieve bar-wave transit time or better. Condition (116) will almost certainly be the case in practice.

Analogous procedures may be applied to the plate elements. *Specifically, Lobatto integration is used on (103), but the factors $t^3/12$ in (102) should be replaced by $tA^e/8$.*

5. Numerical examples

In this section we present several numerical examples which indicate the accuracy attainable by the

reduced integration Lagrange elements. All calculations were performed on the California Institute of Technology, IBM 370/158 computer in double precision (64 bits/floating-point word). Bending moments are reported at 'optimal points' [15] (i.e. the Gauss points of the shear integration rule). A Poisson's ratio of 0.3 and Young's modulus of 10.92×10^5 were used throughout. Generally the meshes are constructed so that there are four U1, or S1, elements for every U2, or S2, element, resulting in the same number of equations. The plates analyzed herein may be considered thin, and so comparison is made with classical thin plate theory. However, since shear deformations are included in the present theory, convergence to slightly greater displacements is to be expected.

5.1. Square plate

Convergence studies were carried out for both simply-supported and clamped, thin, square plates, which were subjected to uniform and concentrated loads. Mesh types are depicted in fig. 8 and results in fig. 9. The geometric data employed were $L = 10$ and $t = 0.1$. Refinements were constructed by bisection. In this problem, the SS_2 simply-supported boundary condition produces convergent solutions and results in fewer equations.

5.2. Circular plate

A convergence study, similar to the preceding one, was carried out for thin circular plates. Meshes are depicted in fig. 10 and the results in fig. 11. The geometric data employed were $R = 5$ and $t = 0.1$. In this case it is necessary to use the SS_1 boundary condition to achieve convergence in the simply-supported case (cf. section 3.4).

Bending moments for elements U1 and S1 are plotted in fig. 12.

5.3. Rhombic plate

The meshes for this problem are depicted in fig. 13. The geometric data employed were $a = 100$ and $t = 0.1$. The plate is simply-supported and subjected to a uniform load. Boundary condition SS_1 is used along the simply-supported edge and, with the exception of U1, the singular behavior of the moments is well repre-

Center displacement normalized with
respect to thin plate theory

Moment at Gauss point nearest center,
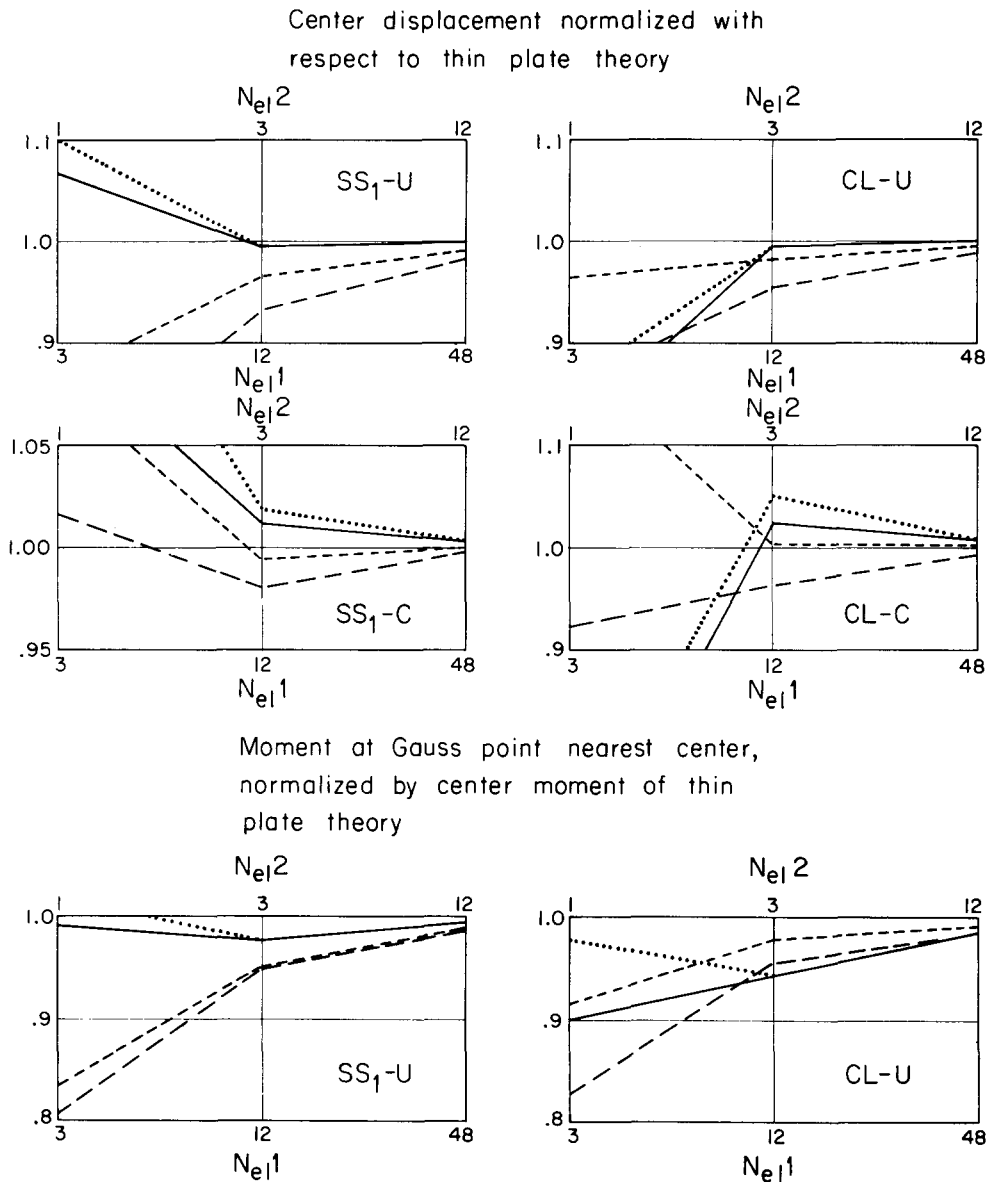normalized by center moment of thin
plate theory

Fig. 11. Convergence study for thin circular plate.

sented (see fig. 14), considering the fact that no effort is made to grade the mesh in favor of the singularity. Element U1 exhibits significant oscillations about the analytical solution, an effect apparently due to the presence of the rotational hourglass modes. Moments for elements U2 and S2, with the exception of one point, are virtually identical.

Many additional applications of reduced integra-

tion plate elements may be found in the papers by Hinton, Zienkiewicz and colleagues (see, e.g. [16–19], and references therein).

6. Conclusions

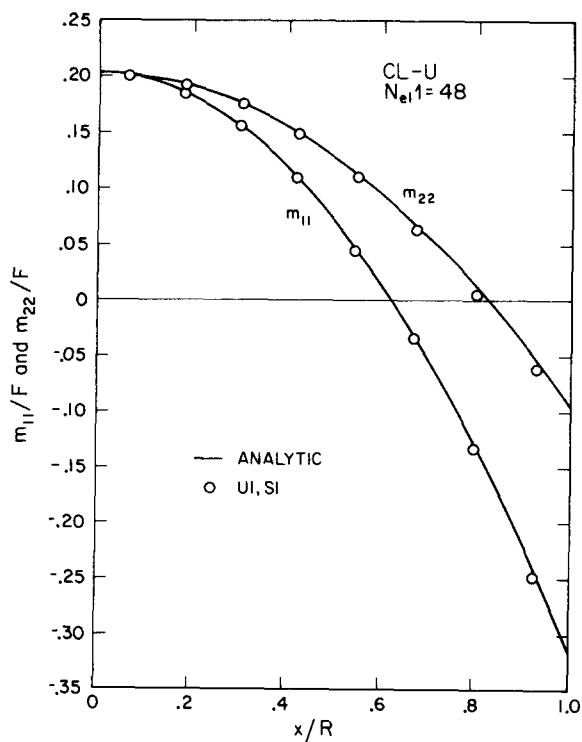The main attributes of the elements presented herein are:

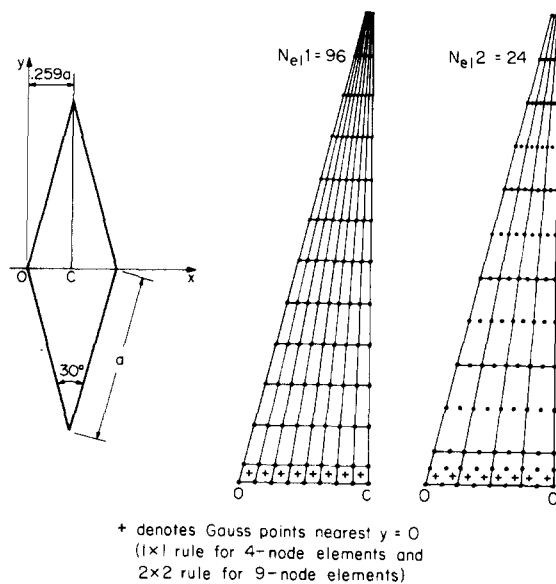Fig. 12. Circular plate. Bending moments at Gauss points nearest x axis.

+ denotes Gauss points nearest $y = 0$
(1×1 rule for 4-node elements and
2×2 rule for 9-node elements)

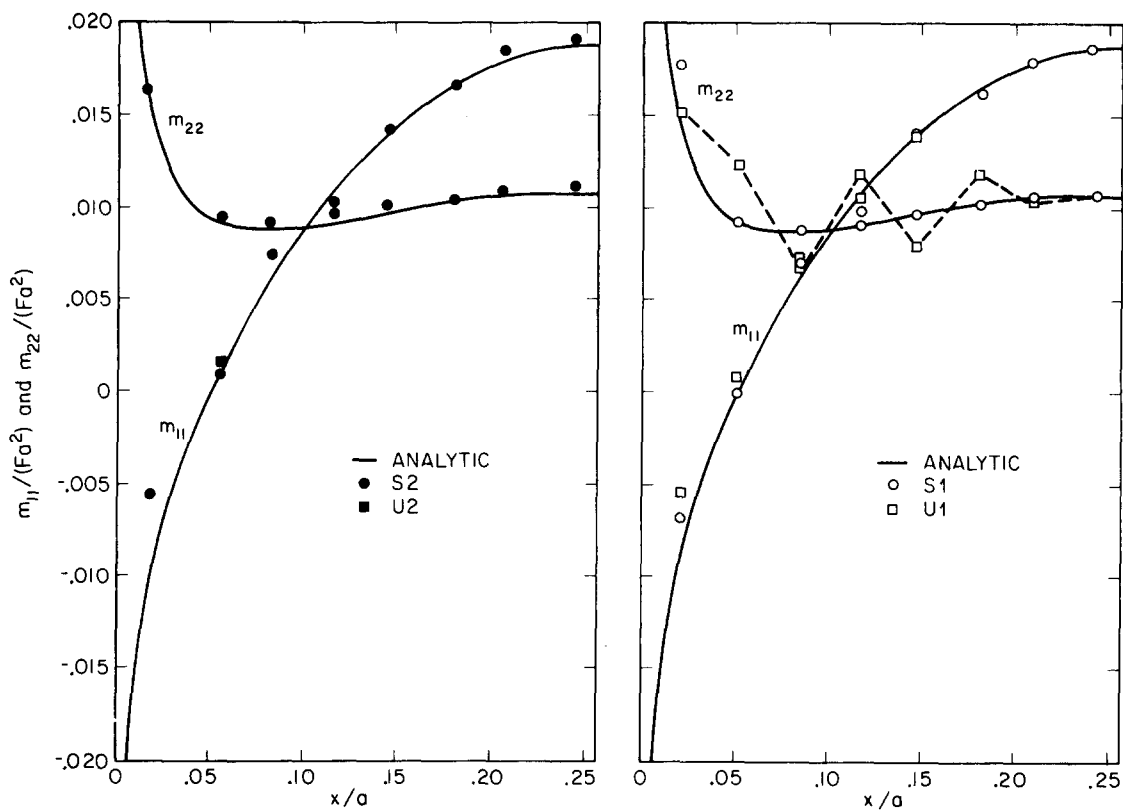Fig. 13. Rhombic plate. Due to symmetry, only one quadrant is discretized.

Fig. 14. Rhombic plate bending moments.

(1) simplicity;

(2) accuracy;

(3) ease of implementation and economy;

(4) the generalization to nonlinear problems is relatively straightforward;

(5) curved, simply-supported boundaries may be treated by polygonal approximations;

(6) singular problems, which have proved insoluble by thin plate elements, are easily handled; and

(7) lumped, positive-definite, mass matrices which yield large critical time steps for explicit transient calculations are simply derived.

The single negative aspect is rank deficiency. In this regard the selectively reduced integration elements are recommended, since they minimize this problem. In our experience S1 seems to be tentatively preferable to S2, since engineering accuracy can generally be obtained somewhat more economically.

If the zero-energy modes can be controlled, the uniform reduced integration elements should be very effective in explicit transient calculations, as they minimize both calculations and storage of stress resultants.

It may be possible to engender further improvements in elements based upon the present theory. The objective is to eliminate the spurious zero-energy modes without adversely affecting convergence. Efforts in this direction are being pursued. One attempt of ours, adding 'incompatible modes' to the four-node element, proved disappointing.

A rather worthwhile endeavor would be to investigate the mathematical basis of the present schemes. There are some delicate questions here.

In assessing the developments described herein, it is not our wish to 'oversell' any of the elements. However, we do believe that, in the hands of capable analysts, these elements are presently among the most effective and versatile tools for the analysis of plates.

Acknowledgements

References

[1] R.D. Mindlin, J. Appl. Mech. 18 (1951) 31.

[2] E.D.L. Pugh, M.Sc. thesis, University College of Swansea, Wales (1976).

[3] T.J.R. Hughes, R.L. Taylor and W. Kanoknukulchai, Int. J. Numer. Methods Eng., 11 (1977) 1529.

[4] E.D.L. Pugh, E. Hinton and O.C. Zienkiewicz, Int. J. Numer. Methods Eng., to appear.

[5] D.S. Malkus and T.J.R. Hughes, Comput. Methods Appl. Mech. Eng., to be published.

[6] O.C. Zienkiewicz, R.L. Taylor and J.M. Too, Int. J. Numer. Methods Eng. 3 (1971) 275.

[7] W.P. Doherty, E.L. Wilson and R.L. Taylor, SESM Report 69-3, Department of Civil Engineering, University of California, Berkeley (1969).

[8] K. Kavanagh and S.W. Key, Int. J. Numer. Methods Eng. 4 (1972) 148.

[9] M. Rossow, J. Appl. Mech. 44 (1977) 347.

[10] L.R. Scott, US–German Symp. on Formulations and Computational Algorithms in Finite Element Analysis, MIT, Cambridge, Mass., 9–13 Aug. 1976.

[11] G. Sander, in: Proc. IUTAM Symp. (Liege, Belgium, 1971) p. 167.

[12] G. Strang and G.J. Fix, An Analysis of the Finite Element Method (Prentice-Hall, Englewood Cliffs, New Jersey, 1973).

[13] I. Fried and D.S. Malkus, Int. J. Solids Struct. 11 (1976) 461.

[14] S.W. Key and Z.E. Beisinger, in: Proc. 3rd Conf. on Matrix Methods in Structural Mechanics (Wright-Patterson Air Force Base, Ohio, 1971).

[15] E. Hinton, A. Razzaque, O.C. Zienkiewicz and J.D. Davies, in: Proc. Inst. Civ. Eng., Part 2, 59 (1975) 43.

[16] J. Barlow, Int. J. Numer. Methods Eng. 10 (1976) 243.

[17] E. Hinton, J. Sound Vib. 46 (1976) 465.

[18] E. Hinton, D.R.J. Owen and D. Shantaram, Conf. on the Mathematics of Finite Elements and Applications II, Brunel University, 1975.

[19] O.C. Zienkiewicz and E. Hinton, J. Franklin Inst. 302 (1976) 443.

Notes added in proof

(1) In our discussion of rank deficiency (see section 3.6) we inadvertently omitted reference to the study of Pian and Mau [20] on thick-plate, "hybrid" elements. Element S1, studied herein, seems to exhibit identical zero-energy mode behavior to the four-node, hybrid element developed in [20].

(2) Professor Atluri has kindly brought to our attention the recent thesis of Rhee [21] in which is discussed the polygonal approximation to simply-sup-

ported, curved-edged, thin plates. Rhee has demonstrated convergence of thin-plate elements for this case by setting boundary-node values of w, but *not* $\partial w/\partial x_\alpha$, equal to zero. This simple technique appears to be the most computationally attractive strategy for overcoming the convergence difficulties described in section 3.4. We note, however, that this approach does not achieve $w = 0$ along the edge of the plate, except in the fine-mesh limit.

(3) We have recently succeeded in developing a high-accuracy, Mindlin-type, plate element without rank deficiency [22].

Additional references

[20] T.H.H. Pian and S.T. Mau, in: Advances in Computational Methods in Structural Mechanics and Design (University of Alabama Press, Huntsville, Alabama, 1972).

[21] H.C. Rhee, Ph.D. thesis, Georgia Institute of Technology, Atlanta (1976).

[22] T.J.R. Hughes and M. Cohen, submitted to Computers and Structures.